NASA TECHNICAL NOTE

NASA TN D-7003

NASA TN D-7003

THEORETICAL AND EXPERIMENTAL VIBRATION AND BUCKLING RESULTS FOR BLUNT TRUNCATED CONICAL SHELLS WITH RING-SUPPORTED EDGES

by Sidney C. Dixon, Robert Miserentino,
and M. Latrelle Hudson

Langley Research Center
Hampton, Va. 23365

NATIONAL AERONAUTICS AND SPACE ADMINISTRATION • WASHINGTON, D. C. • DECEMBER 1970

1. Report No. NASA TN D-7003	2. Government Accession No.	3. Recipient's Catalog No.
4. Title and Subtitle THEORETICAL AND EXPERIMENTAL VIBRATION AND BUCKLING RESULTS FOR BLUNT TRUNCATED CONICAL SHELLS WITH RING-SUPPORTED EDGES		5. Report Date December 1970
		6. Performing Organization Code
7. Author(s) Sidney C. Dixon, Robert Miserentino, and M. Latrelle Hudson		8. Performing Organization Report No. L-7061
		10. Work Unit No. 124-08-20-04
9. Performing Organization Name and Address NASA Langley Research Center Hampton, Va. 23365		
		11. Contract or Grant No.
		13. Type of Report and Period Covered Technical Note
12. Sponsoring Agency Name and Address National Aeronautics and Space Administration Washington, D.C. 20546		
		14. Sponsoring Agency Code

15. Supplementary Notes

16. Abstract

The vibration and buckling characteristics of ring-supported conical shells have been investigated theoretically and experimentally. Theoretical results indicate that rings designed to provide edge restraint between simple and clamped support on the basis of buckling calculations do not provide the equivalent support on the basis of vibration calculations for modes having few circumferential waves. The natural frequencies for these modes were considerably below the minimum frequencies for shells with simply supported or clamped edges. For such cases, studies indicate that substantial increases in ring size and mass are required to effect a significant increase in the minimum frequency of ring-supported shells.

Experimental buckling and vibration results were obtained for four blunt truncated conical shells essentially clamped at the small end and ring-supported at the large end. Buckling was induced by aerodynamic loading in wind-tunnel tests. Theoretical results for the same shells are in good qualitative agreement with the experimental results, but the quantitative agreement is only fair.

17. Key Words (Suggested by Author(s)) Buckling Vibration Conical shells Ring-supported edges	18. Distribution Statement Unclassified — Unlimited		
19. Security Classif. (of this report) Unclassified	20. Security Classif. (of this page) Unclassified	21. No. of Pages 32	22. Price* $3.00

THEORETICAL AND EXPERIMENTAL VIBRATION
AND BUCKLING RESULTS FOR BLUNT TRUNCATED CONICAL SHELLS
WITH RING-SUPPORTED EDGES

By Sidney C. Dixon, Robert Miserentino,
and M. Latrelle Hudson
Langley Research Center

SUMMARY

The vibration and buckling characteristics of ring-supported conical shells have been investigated theoretically and experimentally. Theoretical results indicate that rings designed to provide edge restraint between simple and clamped support on the basis of buckling calculations do not provide the equivalent support on the basis of vibration calculations for modes having few circumferential waves. The natural frequencies for these modes were considerably below the minimum frequencies for shells with simply supported or clamped edges. For such cases, studies indicate that substantial increases in ring size and mass are required to effect a significant increase in the minimum frequency of ring-supported shells.

Experimental buckling and vibration results were obtained from a preliminary investigation of four blunt truncated conical shells essentially clamped at the small end and ring-supported at the large end. Buckling was induced by aerodynamic loading in wind-tunnel tests. Theoretical results for the shells are in good qualitative agreement with the experimental results, but the quantitative agreement is only fair. The rather large differences between theoretical and experimental buckling results are attributed to the large permanent deformations in the shells that resulted from buffeting as the starting shock wave moved down the wind tunnel.

INTRODUCTION

Ring stiffeners are often used to provide edge support for shells of revolution in such aerospace applications as proposed planetary entry vehicles and rocket nozzles. (See refs. 1 and 2.) Since a ring-supported shell may be subjected to both static and dynamic loading, a thorough knowledge of the static and dynamic characteristics of such shell-ring configurations is needed. Recently, there has been considerable theoretical research effort on the buckling of ring-supported shells (e.g., refs. 1 and 3 to 9), but only

limited theoretical results on the free-vibration characteristics of such shells are available (e.g., refs. 2 and 10 to 13); experimental results are even more limited (refs. 6, 12, and 13).

In the present investigation, the buckling and vibration of blunt ring-supported conical shells are considered both theoretically and experimentally. Theoretical vibration results are obtained by use of the approximate theory of reference 7, which treats the vibration, buckling, and flutter of truncated orthotropic conical shells with generalized elastic edge support, such as the restraint imposed by end stiffening rings. The analysis, which uses a Donnell-type shell theory and a membrane prestress state, accounts for the stiffness and inertia characteristics of the end rings in the boundary conditions by use of expressions presented in reference 10. Calculations are presented which show the difference between the vibration characteristics of ring-supported shells and shells with classical edge supports. Additional calculations are presented which indicate the effect of end-ring size on the vibration characteristics of a lightweight entry-vehicle configuration.

Experimental buckling and vibration data were obtained from a preliminary investigation of four blunt cone models essentially clamped at the small end and ring-supported at the large end. The stiffness of the end rings for these models was very close to the minimum stiffness required to provide edge restraint between simple and clamped support on the basis of theoretical buckling calculations. Shell buckling was induced by aerodynamic loading at a Mach number of 3 in the Langley 9- by 6-foot thermal structures tunnel; the vibration data were obtained prior to the wind-tunnel tests. The experimental results are presented and compared with the theoretical predictions in an appendix.

SYMBOLS

The units for the physical quantities defined in this paper are given both in the U.S. Customary Units and in the International System of Units (SI). Appendix A presents factors relating these two systems of units.

A_r cross-sectional area of end ring

$\overline{A}$ nondimensional area parameter, $\overline{A} = E_r A_r \big/ R_1 B$

B extensional stiffness

E Young's modulus of isotropic shell

E_r Young's modulus of end ring

f   frequency

h   wall thickness of isotropic shell

h_c thickness of core of sandwich shell

h_f thickness of face sheet of sandwich shell

I   moment of inertia

I_y, I_z, I_{yz} centroidal moments and product of inertia of ring cross section for conical coordinates

$I_\zeta, I_\xi, I_{\zeta\xi}$ centroidal moments and product of inertia of ring cross section for cylindrical coordinates

$\bar{I}_y, \bar{I}_z, \bar{I}_{yz}$ nondimensional inertia parameters, $\bar{I} = I / R_1^2 A_r$

J   torsion constant for ring cross section

$\bar{J}$ nondimensional torsion-constant parameter, $\bar{J} = J / R_1^2 A_r$

n   number of circumferential waves

p   uniform lateral external pressure

R_1, R_2 radii of conical frustum at small and large end, respectively

r   cross-sectional radius of tubular end ring

t   wall thickness of end ring

v, w   circumferential and normal displacements of middle surface of conical frustum

x   transformed coordinate, $x = \ln(y/y_1)$

$$x_1 = \ln\!\left(y_2/y_1\right)$$

y,z	orthogonal conical coordinates (see fig. 7)
y_1,y_2	distance from vertex to small and large end of cone, respectively
z_0	eccentricity of ring centroidal axis measured from inside shell surface, positive for internal ring
α	semivertex angle of cone
γ	shell density per unit area
μ	Poisson's ratio of isotropic shell
μ_r	Poisson's ratio of end ring
ζ,ξ	orthogonal cylindrical coordinates (see fig. 1)
ρ	density of ring material
$\bar{p}$	nondimensional mass parameter, $\bar{p} = \rho A_r / \gamma R_1$

Subscript:

max	maximum

RESULTS

Analytical results were obtained from the approximate analysis of reference 7. In that analysis, linear Donnell-type equations that utilize the membrane stress state are derived, and the effects of in-plane inertias and prestress deformations are neglected. The resulting equations are solved by an assumed displacement method. In the present investigation, up to 40 terms were used in the computations to insure converged results. Computations were assumed to be converged when the results for N + 4 terms differed by less than 1 percent from the results for N terms.

Calculations are presented for two conical shells previously studied in reference 11 by use of the analysis of reference 10, a rigorous numerical analysis based on Novozhilov shell theory. These calculations are compared with the results of reference 11 to assess

4

the effects of the assumptions in the approximate analysis (ref. 7) used in the present investigation. Additional calculations are presented to show the difference between vibration characteristics of ring-supported shells and shells with classical edge supports and to indicate the effect of ring size on the vibration characteristics of ring-supported conical shells. Experimental buckling and vibration data obtained from a preliminary investigation of blunt cone models essentially clamped at the small end and ring-supported at the large end are given in appendix B. Shell buckling was induced by aerodynamic loading at a Mach number of 3 in the Langley 9- by 6-foot thermal structures tunnel; the vibration data were obtained prior to the wind-tunnel tests.

## Comparison of Results From Donnell and Novozhilov Theories

The vibration characteristics of two designs for a proposed planetary entry capsule were studied in reference 11. The configurations are designated shells A and B herein and are shown, along with pertinent structural data, in figure 1 and table 1. The shells are supported at the large end by an aluminum tubular ring. The section properties of the ring for shell B include both those of the tubular ring and an aluminum channel ring inserted into the end of the sandwich core. Both shell configurations are 120° ($\alpha = 60^O$) truncated cones of aluminum honeycomb sandwich construction. For the purposes of analysis, the sandwich core layer is assumed to provide negligible extensional stiffness while providing sufficient transverse shear and normal stiffness to validate the thin-shell hypothesis of nondeformable normals. The small end of shell A was assumed to be clamped. A payload was assumed to be attached to shell B by an I-section payload ring at the small end of the shell. Calculations for shell B considered the finite stiffness of the payload ring. In addition, the payload mass was uniformly distributed throughout the payload ring by increasing the ring density in such a manner that the ring mass equaled the total mass of the payload and attachment. In order to account for the mass of a heat-shield layer, a surface density of 0.70 lbm/ft^2 (3.42 kg/m^2) was added to the surface density of the structural sandwich to obtain the total density of the shell wall for both shells.

In figure 2, the natural frequencies of shells A and B determined from the theory of the present investigation (solid lines) are compared with the results of reference 11 (circles); the results of reference 11 were calculated from the theory of reference 10. In view of the limitations of the Donnell theory, results from the present investigation are presented only for n ≧ 2. The results in figure 2(a) are for a shell clamped at the small end and ring-supported at the large end (shell A), whereas the results in figure 2(b) are for a shell with rings on both ends (shell B). As can be seen in figure 2, the frequencies obtained from the present (modal) analysis are in good agreement with the frequencies obtained from the more rigorous (numerical) analysis of reference 10, which is based on Novozhilov shell theory. The differences are from about 1 to 7 percent for

shell A (clamped/ring support) and from about 5 to 12 percent for shell B (ring/ring support). Thus, the theory of reference 7 appears to be adequate for studies of the vibration characteristics of blunt ring-supported isotropic shells.

Effects of Size of End Rings

In most studies of ring-supported conical shells, the end rings have been designed on the basis of buckling considerations. (See, for example, ref. 11.) The buckling characteristics of ring-supported shells are indicated in sketch (a). As can be seen, buckling of shells with end rings may occur in either of two modes: If the rings are not very stiff, the shell buckles almost inextensionally into very few circumferential waves (usually 2 or 3) at loads which vary considerably with ring stiffness, and which can be several orders of magnitude smaller than the buckling loads for clamped shells (ref. 4). If the ring is sufficiently stiff, the shell buckles extensionally into a higher number of circumferential waves at loads bracketed by the buckling loads for simply supported and clamped edges; these loads do not vary significantly with ring stiffness. Use of the smallest (lightest) ring required to suppress the inextensional form of buckling generally results in minimum total mass of the shell and ring for a shell designed to withstand buckling. (See ref. 9.) This design philosophy was used in the design of the end rings for shells A and B. To determine the effectiveness of these rings on the basis of vibration calculations, the natural frequencies for the same shells with various classical boundary conditions were
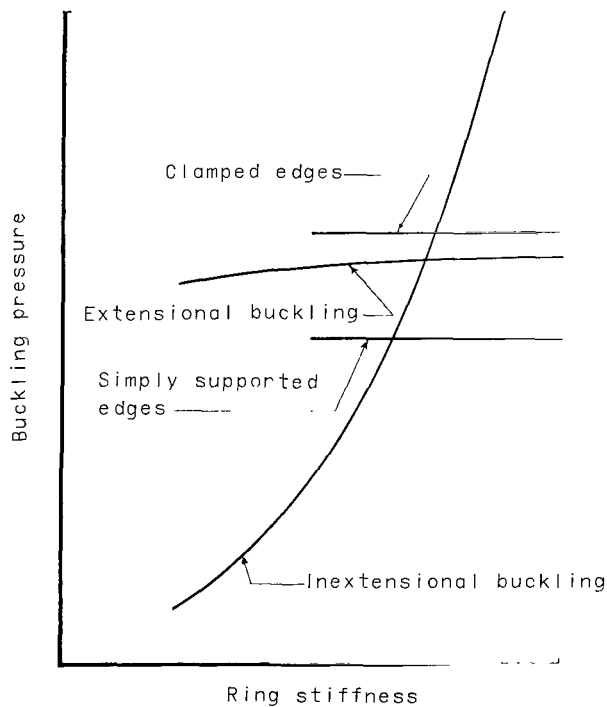
Sketch (a)

obtained for comparison with the frequencies for the ring-supported shells. The results are presented in figure 3. The solid curves are for ring-supported shells, the short-dash curves are for shells with both edges simply supported, and the long-dash curves are for shells with both edges clamped. As can be seen in the figure, the results for clamped and supported edges indicate the minimum frequency occurs for $n = 4$. For $n > 4$, the results for ring-supported shells are bracketed by the results for clamped and simply supported shells. However, for $n < 4$, the results for ring-supported shells fall well below the results for clamped or simply supported shells and indicate the minimum frequency occurs at $n = 2$. Thus, a ring designed to provide edge restraint between simply supported and clamped on the basis of buckling calculations does not provide the equivalent support on the basis of vibration calculations for small values of n, and ring stiffness must be considered in calculations for these modes.

The mode shapes for shell B (ring/ring support) and for a clamped shell are indicated in figure 4. The shell with ring support vibrates in essentially an inextensional mode for $n = 2$, with the maximum amplitude occurring at the large end of the cone (fig. 4(a)). Either of the edge restraints $v = 0$ or $w = 0$, which apply to both simple and clamped support, suppresses the inextensional mode of vibration. For higher values of n, the inextensional mode does not occur for the ring-supported shell, and the mode shapes approach those for the fully clamped shell. (See figs. 4(d) to 4(f).) Similar trends for a conical shell clamped on the small end and ring-supported on the large end are presented in reference 2.

The very low frequencies that occur for low values of n may result in the undesirable dynamic response of, for example, an entry vehicle in the launch configuration subjected to the launch vibration environment. Calculations were therefore made to determine the effect of increases in the size of the base ring on the frequency results for shell A. Frequency results for $n = 2$ and $n = 4$ for various values of r/R_2 are shown in figure 5. In order to investigate the effects of both the finite-coupled elastic restraint of the ring and the inertia loading of the vibrating ring mass, calculations were made for rings with a density ρ corresponding to aluminum (solid curves) and also with $\rho = 0$ (dashed curves). The ratio of the ring cross-section radius to ring thickness was kept constant at $r/t = 34.4$, the value corresponding to the original base ring.

The results of figure 5 indicate that the effect of the inertial force of the vibrating ring mass was small for $r/R_2 = 0.0294$, the size of the original base ring. As the ratio r/R_2 increases, the effect of ring mass decreases for $n = 4$ but increases for $n = 2$. The minimum frequency for the ring-supported shell occurs in the $n = 2$ mode when $\frac{r}{R_2} < 0.11$ and occurs in the $n = 4$ mode when $\frac{r}{R_2} \geqq 0.11$; further increases in ring size do not significantly alter this minimum frequency. For $\frac{r}{R_2} > 0.088$, the minimum

frequency for the ring-supported shell is bracketed by the minimum frequencies for the shells with simple and clamped supports.

The total mass of the ring for $r/R_2 = 0.088$ is over eight times the mass of the ring for $r/R_2 = 0.0294$. Thus, increasing the minimum frequency of ring-supported shells by increasing the size of the base ring can result in a significant increase in base-ring mass. The variation of the mode shapes with r/R_2 is shown in figure 6. For $r/R_2 = 0.0294$ and $r/R_2 = 0.0555$, the shell vibrates in essentially an inextensional mode with $n = 2$. For $r/R_2 = 0.1670$, the vibration mode has become extensional but still differs somewhat from the mode for the shell with clamped edges.

The theoretical results presented in figures 3 and 5 indicate that rings designed to provide edge restraint between simply supported and clamped on the basis of buckling calculations do not provide the equivalent support on the basis of vibration calculations. Results of the preliminary experimental investigation described in appendix B tend to verify these trends. Appendix B also shows that theoretical results for the shells are in good qualitative agreement with the experimental data but that the quantitative agreement is only fair. The differences between theoretical and experimental buckling results are attributed to the large permanent deformations in the shells that resulted from buffeting as the starting shock wave moved down the wind tunnel.

CONCLUDING REMARKS

The vibration and buckling characteristics of ring-supported conical shells have been investigated theoretically and experimentally. Theoretical results indicate that rings designed to provide edge restraint between simple and clamped support on the basis of buckling calculations do not provide the equivalent support on the basis of vibration calculations for modes having few circumferential waves. The natural frequencies for these modes were considerably below the minimum frequencies for shells with simple and clamped support edges. For such cases, the present study indicates that substantial increases in ring size and mass are required to effect a significant increase in the minimum frequency of ring-supported shells.

Experimental buckling and vibration data were obtained from a preliminary investigation of four blunt truncated conical shells essentially clamped at the small end and ring-supported at the large end. Buckling was induced by aerodynamic loading in wind-tunnel tests. Theoretical results for the shells are in good qualitative agreement with the experimental data, but the quantitative agreement is only fair. The rather large differences between theoretical and experimental buckling results are attributed to the large

permanent deformations in the shells that resulted from buffeting as the starting shock wave moved down the wind tunnel.

Langley Research Center,
     National Aeronautics and Space Administration,
          Hampton, Va., October 16, 1970.

APPENDIX A

CONVERSION OF U.S. CUSTOMARY UNITS TO SI UNITS

The International System of Units (SI) was adopted by the Eleventh General Conference on Weights and Measures, Paris, October 1960. (See ref. 14.) Conversion factors for the units used herein are given in the following table:

Physical quantity	U.S. Customary Unit	Conversion factor (*)	SI Unit (**)
Area	in^2	0.6452×10^{-3}	meters^2 (m2)
Length	in.	0.0254	meters (m)
Mass/area	lbm/ft^2	4.882	kilograms/meter^2 (kg/m2)
Mass density	lbm/in^3	2.768×10^4	kilograms/meter^3 (kg/m3)
Moment of inertia.	in^4	0.4162×10^{-6}	meters^4 (m4)
Pressure	psi = lbf/in^2	6.895×10^3	newtons/meter^2 (N/m2)
	lbf/ft^2	4.788×10	newtons/meter^2 (N/m2)
Young's and shear moduli . .	lbf/in^2	6.895×10^3	newtons/meter^2 (N/m2)
Temperature	$^{\circ}F$	$\dfrac{^{\circ}F + 459.67}{1.8}$	kelvins (K)

*Multiply value given in U.S. Customary Units by conversion factor to obtain equivalent value in SI Units.

**Prefixes to indicate multiples of units are as follows:

Prefix	Multiple
giga (G)	10^9
kilo (k)	10^3
centi (c)	10^{-2}
milli (m)	10^{-3}

APPENDIX B

PRELIMINARY EXPERIMENTAL INVESTIGATION

Since experimental data for vibration or buckling of ring-supported shells are very limited, a preliminary experimental investigation was conducted to provide additional experimental data and trends.

Models

The models were blunt truncated conical shells with a radius ratio R_2/R_1 of 2.544. Two models had a semivertex angle α of 60° and nominal large radius thickness ratio R_2/h of 132. For the other two models, $\alpha = 70^\circ$ and $R_2/h = 118$. Each model was machined from a solid piece of magnesium. Construction details, material properties, and dimensions of the models are given in figure 7. A solid spherical nose cap was rigidly attached to a mounting sting in such a manner that the small end of each model was essentially clamped. The large end was supported by an integral end ring; properties of the end rings are given in figure 7. The stiffness of the end rings for the models was very close to the minimum stiffness required to provide restraint between simply supported and clamped at the large end of the shell on the basis of theoretical buckling calculations.

Test Technique

Vibration tests.- The models were sting mounted in the wind-tunnel test section (fig. 8) and were vibrated prior to the wind-tunnel tests. The models were excited with an air-jet shaker, which is described in reference 15. The frequency was varied between 5 and 1000 Hz until an increased response indicated a natural frequency. The force applied was then increased, and a contact accelerometer was moved manually about the shell outer surface until the positions of the node lines were located. The frequency was determined by an electronic counter, which sampled the accelerometer output.

Buckling tests.- Buckling was induced by aerodynamic loading; the buckling tests were conducted in the Langley 9- by 6-foot thermal structures tunnel, which is a Mach 3 blowdown facility exhausting to the atmosphere. The tunnel stagnation-pressure operating range is from 50 to 200 psia (380 to 1380 kN/m^2). A complete description of the facility is given in reference 16. The models were subjected to severe buffeting as the starting shock wave moved down the wind tunnel during tunnel startup. The models were supported by retractable support vanes during tunnel startup to minimize the effect of the buffeting. Figure 8 is a photograph of the test section prior to a test; it shows the model in place, the model support vanes partially retracted, the sting, and the sting support. The tunnel

was started at the minimum dynamic pressure of 1480 lbf/ft^2 (71 kN/m^2) with the sting-mounted model supported from behind by the eight retractable support vanes. Once the flow was established, the vanes were retracted 30 inches (76 cm), and the dynamic pressure was then increased until buckles were seen. The stagnation temperature for all tests was 200° F (366 K).

Each of the four models was tested once; the longest test lasted about 26 seconds. Recorded data consisted of motion pictures taken at 400 frames per second, base pressures, tunnel pressures, model temperature, and axial force. The external pressure p acting on the shell was assumed to be uniform and adequately given by the magnitude of the total axial force divided by the total frontal area of the model. Results presented in reference 17 indicate that the pressure on a 120° cone varies smoothly along the cone meridian; maximum variation from the average pressure was of the order of 10 percent. Use of the results of reference 17 in conjunction with the measured base pressures gave essentially the same values for the external pressure as obtained from the axial-force measurements.

Results

Vibration results.- The measured resonant frequencies for the recorded modes (for one half-wave in the longitudinal direction) are given in table 2. The minimum frequency occurs at n = 3 for the 120° cones and at n = 2 for the 140° cones. The overall trends are similar to the trends presented in references 18 and 19 for clamped/free shells. The larger end ring (ring 2) generally increased the frequencies only slightly and actually decreased the frequency for the 120° cone at n = 2.

Buckling results.- The measured buckling pressure and circumferential wave number n are given in table 3 for each shell. All shells suffered permanent deformation (fig. 9) due to buffeting as the starting shock wave moved down the wind tunnel during tunnel startup. The 120° cone with ring 1 was so damaged that the end ring was permanently deformed, and the model failed immediately after the supporting vanes were retracted, at a pressure lower than those for the other three models (table 3). The other three shells were visibly deformed into an n = 8 mode (fig. 9) by the eight model support vanes, but the end rings were essentially undeformed. These large prebuckling deformations undoubtedly affected the buckling load and modes. Even though the quality of the data was adversely affected by the test technique, the data are presented because of the uniqueness of the tests, which simulated the type of loading on planetary entry vehicles.

The shell deformations were most severe for the shells with the smaller cone angle (also smaller shell thickness, fig. 7) and the smaller end rings. The shells with the smaller end rings (ring 1) appeared to buckle initially into an n = 4 mode; the shells

with the larger rings (ring 2) buckled at higher pressures into an $n = 7$ mode. All shells ultimately collapsed into an $n = 3$ mode as dynamic pressure was increased; a photograph of a collapsed model is shown in figure 10.

Comparison of Theory and Experiment

Vibration results.- Theoretical and experimental vibration results are shown in figure 11 in terms of the shell frequencies and wave number n. The curves represent theoretical results for various classical boundary conditions, a clamped edge at the small end and either a clamped, simply supported, or free edge at the large end; the symbols are for clamped/ring support; and the solid symbols represent experimental data. At $n = 2$ or 3 the theoretical effects of the rings are slight, and the shells vibrate essentially as a clamped/free shell. As n increases, the effect of the rings becomes more pronounced, and for $n > 7$, the frequencies are bracketed by the frequencies for clamped/ supported and clamped/clamped edges. The theoretical effect of the increase in ring size is slight.

The theory predicts the correct value of n for the minimum frequency for each shell, and the theoretical and experimental results are in good qualitative agreement for the entire range of n considered. However, the quantitative agreement is only fair. Excluding $n = 2$, the largest difference between theoretical and experimental results was 26 percent; experimental frequencies were generally less than the results predicted by theory. The theoretical and experimental vibration results reveal that the end rings did not provide edge restraint between simply supported and clamped for $n < 7$. In fact, at $n = 2$, the experimental data differ from the theoretical frequencies for clamped or supported edges by a factor of 4 for the 120° cone and by nearly an order of magnitude for the 140° cone.

Buckling results.- Theoretical and experimental buckling results are shown in figure 12 where buckling pressure is shown as a function of circumferential wave number n. In the theoretical calculations, each shell was subjected to lateral external pressure, and static equilibrium was maintained by an axial load applied at the small end of the cone, as indicated by the sketch in the figure. The solid curves represent theoretical results for various classical boundary conditions, clamped at the small end and either clamped, simply supported, or free at the large end; the symbols are for shells clamped at the small end and ring-supported at the large end; experimental data are indicated by the solid symbols. The results for shells with classical edge support indicate for each shell a single minimum value of pressure, which occurs at $n = 8, 7$ $(120^\circ, 140^\circ)$ for shells with either clamped or simply supported edges at the large end and at $n = 5, 4$ $(120^\circ, 140^\circ)$ for shells with a free edge at the large end. However, the results for ring support indicate two relative minimums, one at $n = 3$ and one at $n = 7$. The lowest theoretical

buckling pressure occurs at $n = 3$ for the 140° cone with ring 1 and at $n = 7$ for the other three shell-ring configurations. As can be seen in figure 12, the theoretical minimum buckling pressure for each ring-supported shell is approximately the same as the buckling pressure for the shells with clamped/simply supported edges.

The large differences in the theoretical and experimental results are attributed to the large visible permanent deformations in the shells that resulted from buffeting as the starting shock wave moved down the wind tunnel. The 120° cone with ring 1 was so damaged that the end ring was permanently deformed; therefore, a meaningful comparison with theory was precluded. The other three shells were deformed into an $n = 8$ mode, but the end rings were essentially undeformed. Results for the 140° cone (fig. 12(b)) reveal that the larger ring (ring 2) caused an increase in buckling pressure and circumferential wave number. These results agree with the theoretical trend. The experimental data range from 44 percent to 58 percent of the theoretical results. Typical experimental data for the static buckling of shells with no readily visible imperfections subjected to pressure loading under laboratory conditions range from 60 percent to 140 percent of the values predicted for simply supported ends (ref. 20); the lower experimental values are attributed primarily to initial imperfections (ref. 20). Thus, considering the large initial imperfections of the test models of this investigation, the differences between theory and experiment are not unrealistic.

The theoretical results presented in figure 12 were obtained from the approximate theory of reference 7. To determine the effect of the approximations in this analysis (Donnell theory, membrane prestress, and neglect of prestress deformations), calculations were made for the 120° cone with ring 1 by use of a rigorous numerical analysis which was recently completed at the Langley Research Center. The analysis, which is based on Sanders shell theory, and the corresponding computer program SALORS (Structural Analysis of Layered Orthotropic Ring-Stiffened Shells), although not fully documented in the literature, are briefly described in reference 21. Accurate prestress quantities obtained from the stress analysis section of the computer program were used as input for the buckling calculations. The buckling results obtained from SALORS differed by about 2 percent or less from the results obtained from the analysis of reference 7 except at $n = 2$ where significant differences between Sanders and Donnell theory are expected. Thus, the approximations in the analysis of reference 7 had only a slight effect on the accuracy of the results presented in figure 12.

REFERENCES

1. Cohen, Gerald A.: The Effect of Edge Constraint on the Buckling of Sandwich and Ring-Stiffened 120 Degree Conical Shells Subjected to External Pressure. NASA CR-795, 1967.

2. Newton, R. A.: Free Vibrations of Rocket Nozzles. AIAA J., vol. 4, no. 7, July 1966, pp. 1303-1305.

3. Almroth, B. O.; and Bushnell, D.: Computer Analysis of Various Shells of Revolution. AIAA J., vol. 6, no. 10, Oct. 1968, pp. 1848-1855.

4. Cohen, Gerald A.: Buckling of Axially Compressed Cylindrical Shells With Ring-Stiffened Edges. AIAA J., vol. 4, no. 10, Oct. 1966, pp. 1859-1862.

5. Bushnell, David: Buckling of Spherical Shells Ring-Supported at the Edges. AIAA J., vol. 5, no. 11, Nov. 1967, pp. 2041-2046.

6. Wang, Leon Ru-Liang: Effects of Edge Restraint on the Stability of Spherical Caps. AIAA J., vol. 4, no. 4, Apr. 1966, pp. 718-719.

7. Dixon, Sidney C.; and Hudson, M. Latrelle: Flutter, Vibration, and Buckling of Truncated Orthotropic Conical Shells With Generalized Elastic Edge Restraint. NASA TN D-5759, 1970.

8. Bushnell, David: Inextensional Buckling of Spherical Shells With Edge Rings. AIAA J., vol. 6, no. 2, Feb. 1968, pp. 361-364.

9. Dixon, Sidney C.; and Carine, John B.: Preliminary Design Procedure for End Rings of Isotropic Conical Shells Loaded by External Pressure. NASA TN D-5980, 1970.

10. Cohen, Gerald A.: Computer Analysis of Asymmetric Free Vibrations of Ring-Stiffened Orthotropic Shells of Revolution. AIAA J., vol. 3, no. 12, Dec. 1965, pp. 2305-2312.

11. Cohen, Gerald A.; Foster, Richard M.; and Schafer, Everett M.: Analysis of Conceptual Designs for the Voyager Entry Capsule. Contract No. NAS1-5554-1, Philco-Ford Corp. (Available as NASA CR-66580.)

12. Sewall, John L.; and Catherines, Donnell S.: Analytical Vibration Study of a Ring-Stiffened Conical Shell and Comparison With Experiment. NASA TN D-5663, 1970.

13. Steeves, Earl C.; Durling, Barbara J.; and Walton, William C., Jr.: A Method for Computing the Response of a General Axisymmetric Shell With an Attached Asymmetric Structure. AIAA Structural Dynamics and Aeroelasticity Specialist Conference and the ASME/AIAA 10th Structures, Structural Dynamics, and Materials Conference, Apr. 1969, pp. 302-328.

14. Comm. on Metric Pract.: ASTM Metric Practice Guide. NBS Handbook 102, U.S. Dep. Com., Mar. 10, 1967.

15. Herr, Robert W.: A Wide-Frequency-Range Air-Jet Shaker. NACA TN 4060, 1957.

16. Schaefer, William T., Jr.: Characteristics of Major Active Wind Tunnels at the Langley Research Center. NASA TM X-1130, 1965.

17. Stallings, Robert L., Jr.; and Tudor, Dorothy H.: Experimental Pressure Distributions on a 120° Cone at Mach Numbers From 2.96 to 4.63 and Angles of Attack From 0° to 20°. NASA TN D-5054, 1969.

18. Weingarten, V. I.: Free Vibrations of Conical Shells. J. Eng. Mech. Div., Amer. Soc. Civil Eng., vol. 91, no. EM 4, Aug. 1965, pp. 69-87.

19. Weingarten, Victor I.; and Gelman, Alfred P.: Free Vibrations of Cantilevered Conical Shells. J. Eng. Mech. Div., Amer. Soc. Civil Eng., vol. 93, no. EM 6, Dec. 1967, pp. 127-138.

20. Seide, Paul: A Survey of Buckling Theory and Experiment for Circular Conical Shells of Constant Thickness. Collected Papers on Instability of Shell Structures — 1962, NASA TN D-1510, 1962, pp. 401-426.

21. Anderson, M. S.; Fulton, R. E.; Heard, W. L., Jr.; and Walz, J. E.: Stress, Buckling, and Vibration Analysis of Shells of Revolution. NASA paper presented at Conference on Computer Oriented Analysis of Shell Structures (Palo Alto, Calif.), Aug. 1970.

TABLE 1.- MODEL PROPERTIES

(a) Shell A.

Shell properties:

h_f . . . . 0.016 in. (0.041 cm)

h_c . . . . 0.530 in. (1.35 cm)

γ . . . . 1.469 lbm/ft^2 (7.172 kg/m^2)

E . . . . 10.5 × 10^6 lbf/in^2 (72.4 GN/m^2)

μ 0.32

Ring properties:

r . . . . 2.65 in. (6.73 cm)

t . . . . 0.077 in. (0.196 cm)

A_r . . . . 1.28 in^2 (8.26 cm^2)

I_ζ, I_ξ, J/2 . . . . 4.45 in^4 (185.2 cm^4)

$I_{\zeta\xi}$ 0

z_o . . . . 2.70 in. (6.86 cm)

E_r . . . . E

μ_r . . . . μ

ρ . . . . 0.1 lbm/in^3 (2768.0 kg/m^3)

(b) Shell B.

Shell properties:

h_f . . . . 0.020 in. (0.051 cm)

h_c . . . . 0.75 in. (1.91 cm)

γ . . . . 1.714 lbm/ft^2 (8.368 kg/m^2)

E . . . . 10.5 × 10^6 lbf/in^2 (72.4 GN/m^2)

μ 0.32

Ring properties:

Small end:

A_r . . . . 0.648 in^2 (4.18 cm^2)

I_ζ . . . . 0.517 in^4 (21.5 cm^4)

I_ξ . . . . 1.058 in^4 (44.0 cm^4)

$I_{\zeta\xi}$ . . . . -0.45 in^4 (-18.7 cm^4)

J . . . . 0.1045 × 10^{-3} in^4 (4.35 × 10^{-3} cm^4)

z_o . . . . 0.805 in. (2.04 cm)

E_r . . . . E

μ_r . . . . μ

ρ . . . . 151.7 lbm/in^3 (4.2 Gg/m^3)

Large end:

A_r . . . . 1.8 in^2 (11.6 cm^2)

I_ζ . . . . 9.9 in^4 (412.0 cm^4)

I_ξ . . . . 11.6 in^4 (482.8 cm^4)

$I_{\zeta\xi}$ . . . . -1.25 in^4 (-52.0 cm^4)

J . . . . 18.45 in^4 (767.9 cm^4)

z_o . . . . 3.01 in. (7.64 cm)

E_r . . . . E

μ_r . . . . μ

ρ . . . . 0.1 lbm/in^3 (2768.0 kg/m^3)

TABLE 2.- EXPERIMENTAL FREQUENCIES OF RING-SUPPORTED SHELLS

n	f, Hz			
	120° cone		140° cone	
	Ring 1	Ring 2	Ring 1	Ring 2
2	271	261	141	146
3	249	258	247	253
4	302	324	343	370
5		576	478	512
6			608	
7	860	882	838	865

TABLE 3.- EXPERIMENTAL BUCKLING LOADS FOR RING-SUPPORTED SHELLS

Shell, deg	Ring	n at –		p	
		Buckle	Collapse	psi	kN/m^2
140	1	4	3	19.1	131.7
140	2	7	3	23.5	162.0
120	1	4	3	[a]14.9	[a]102.7
120	2	7	3	18.9	130.3

[a]Shell end ring damaged during tunnel startup.
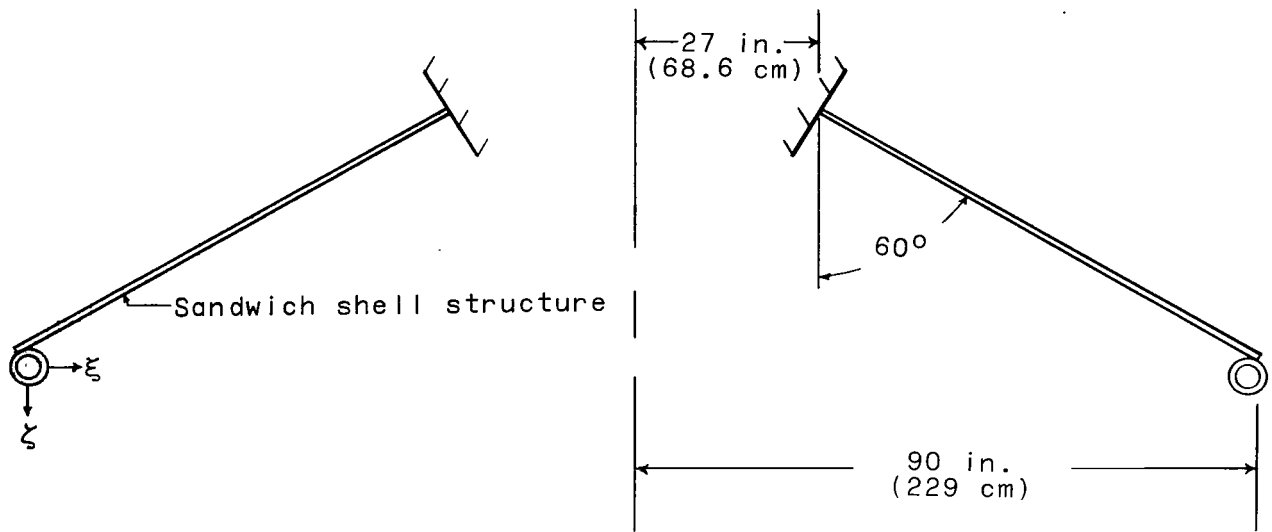
(a) Shell A.
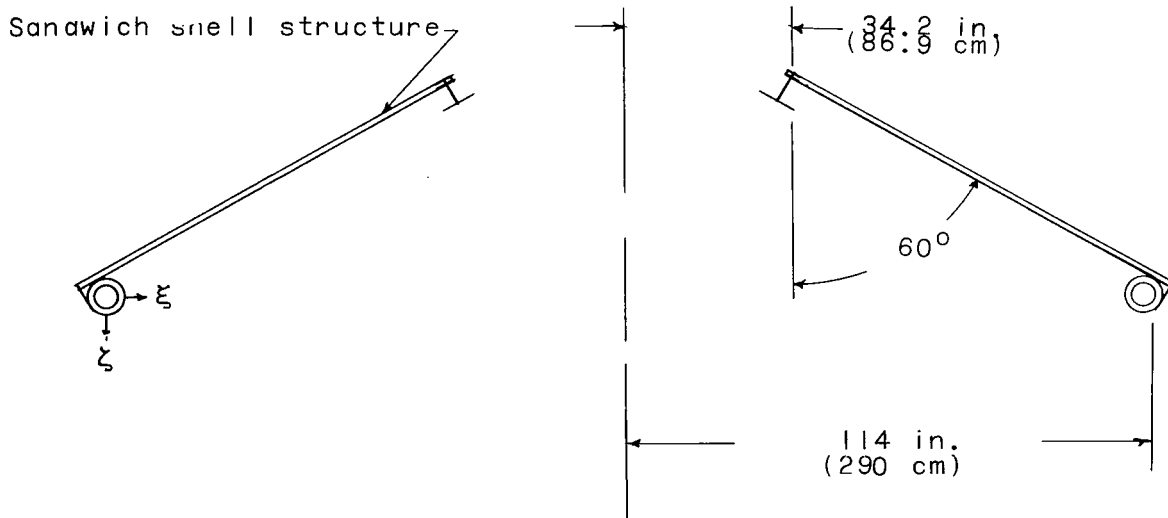
(b) Shell B.

Figure 1.- Idealized configurations of designs for proposed entry vehicle.
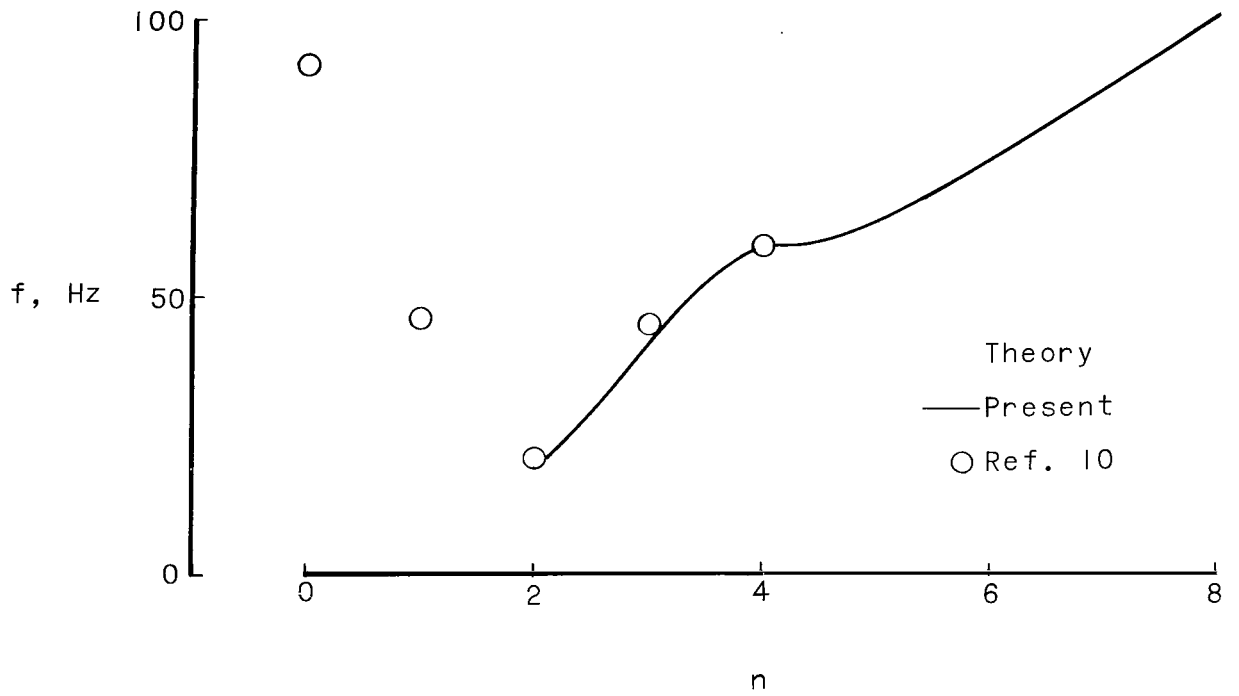
(a) Shell A.
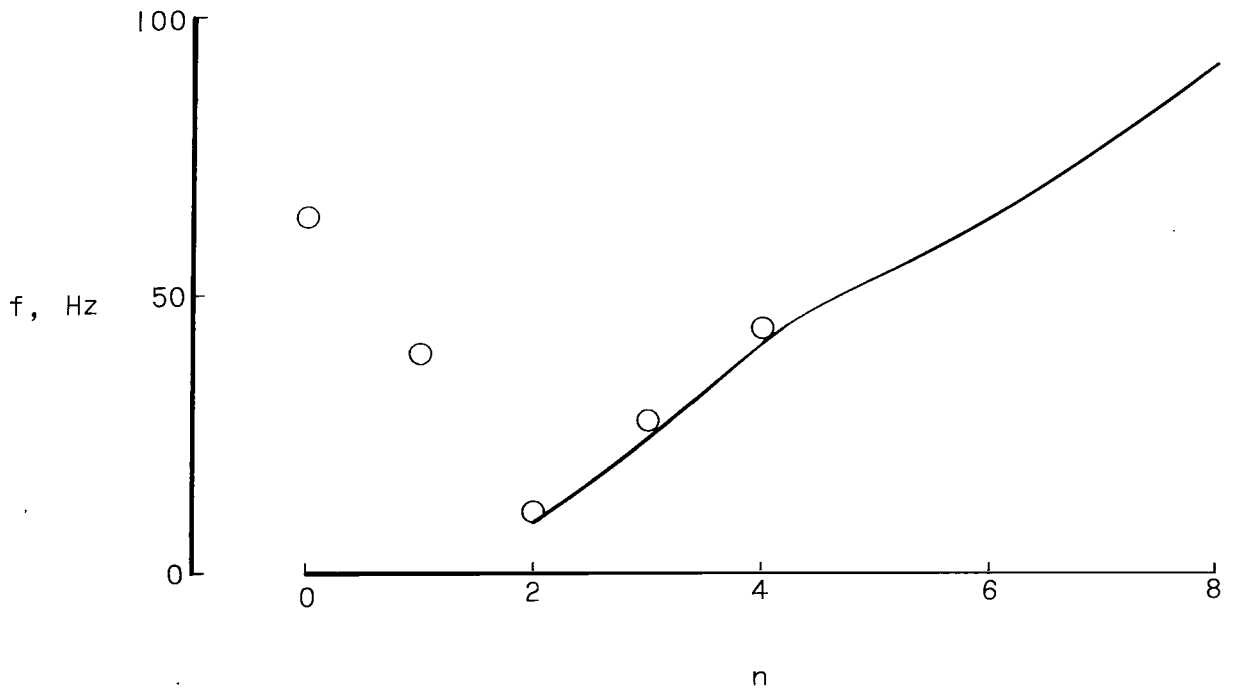
(b) Shell B.

Figure 2.- Free-vibration characteristics of conical shells with
ring-supported edges.   (See fig. 1 for shell geometry.)
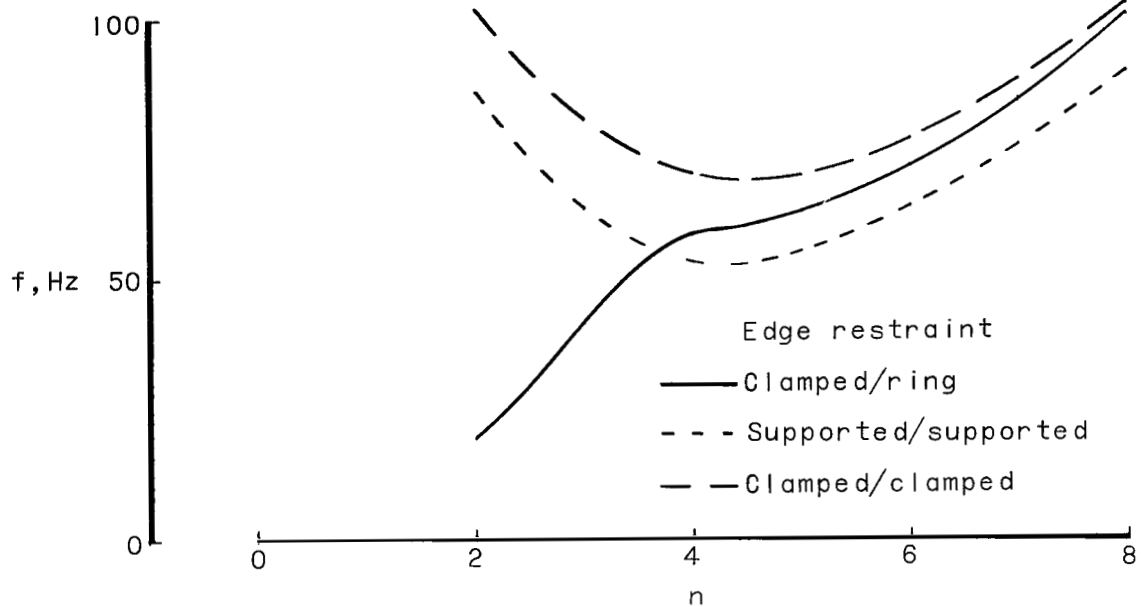
(a) Shell A.
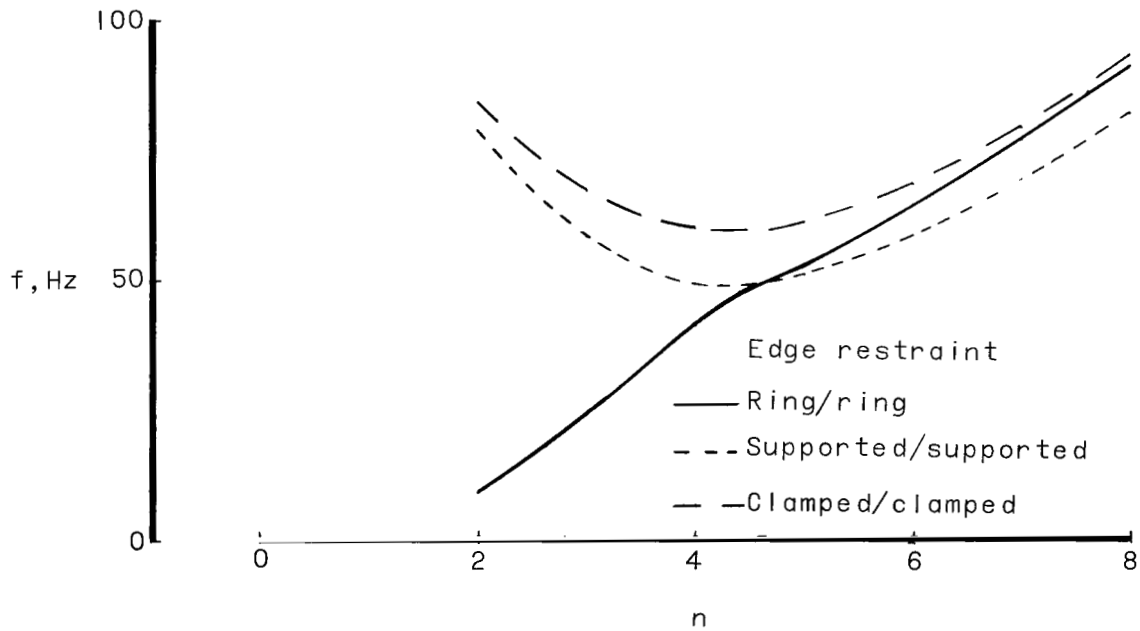
(b) Shell B.

Figure 3.- Effects of edge support on free-vibration characteristics of conical shells. (See fig. 1 for shell geometry.)
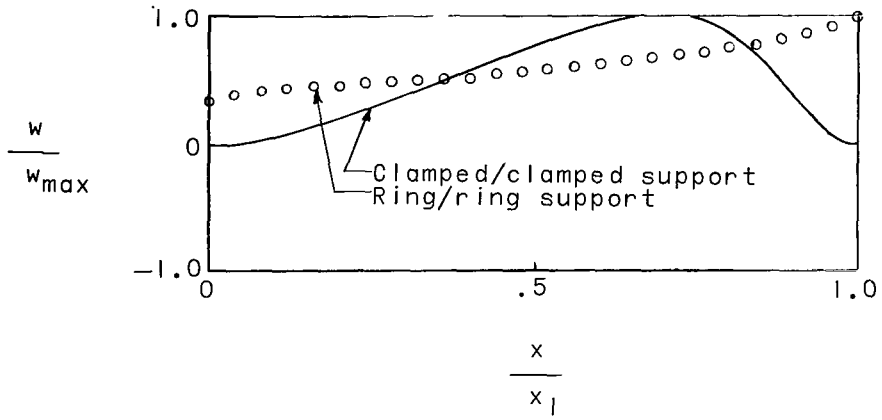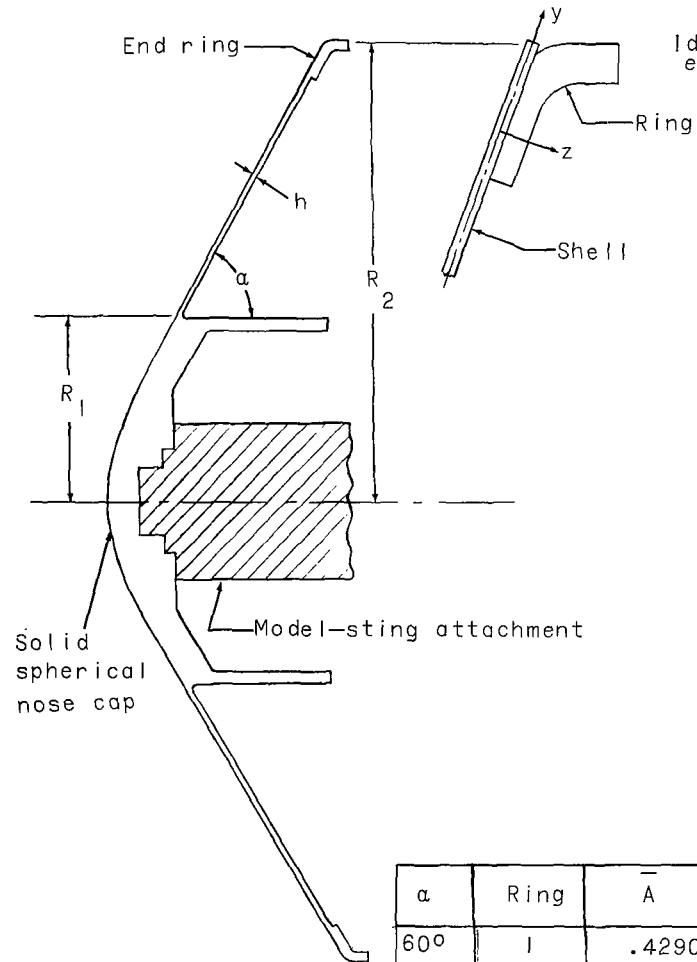
(a) n = 2.
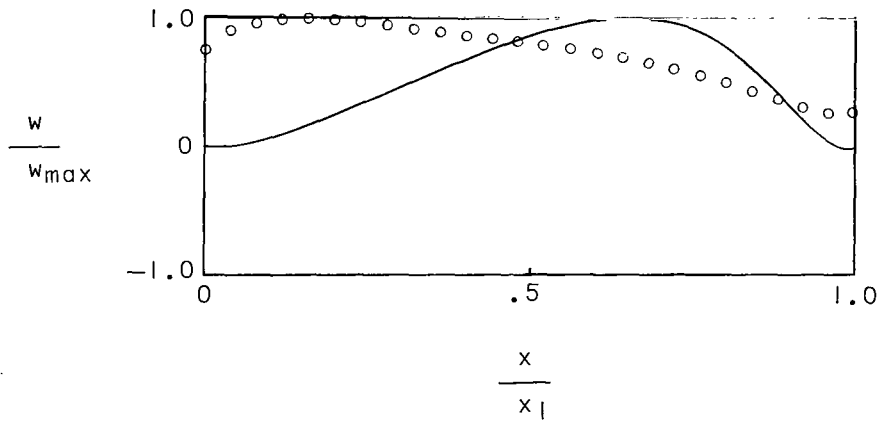
(b) n = 3.
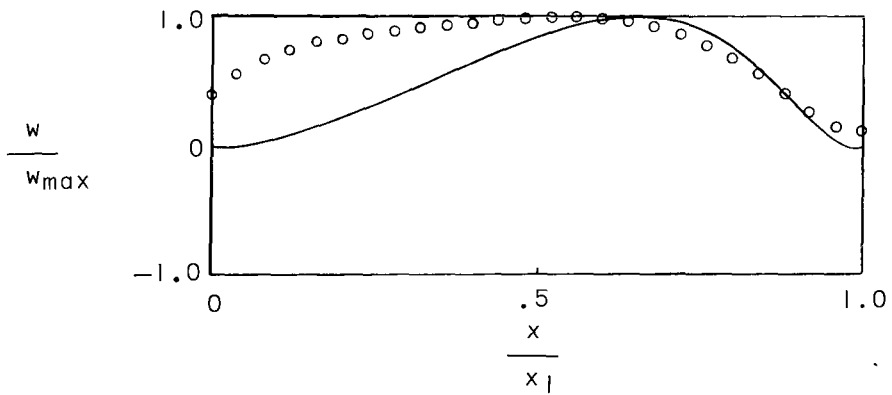
(c) n = 4.

Figure 4.- Vibration mode shapes for shell B.
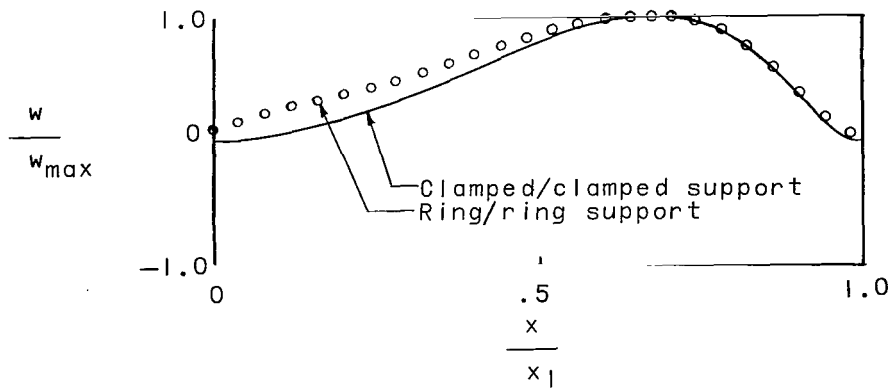
(d) n = 5.
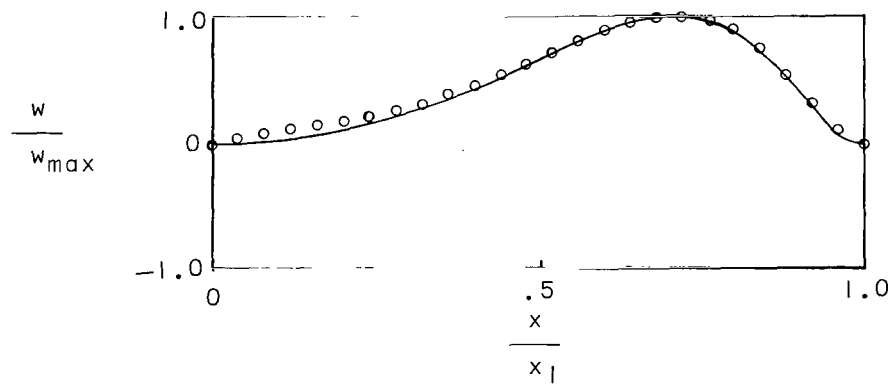
(e) n = 6.
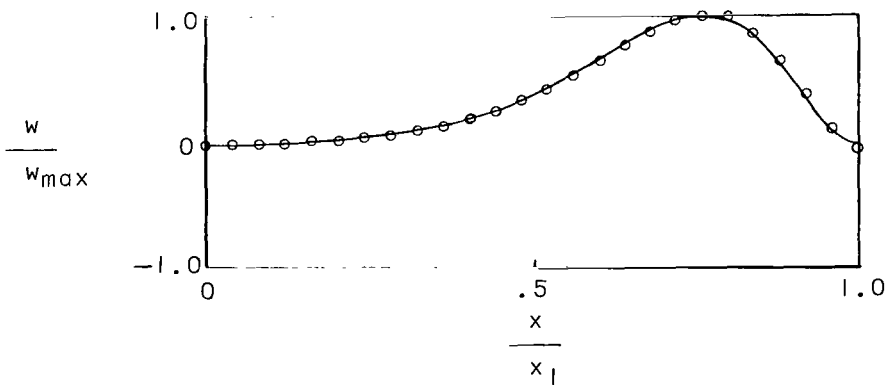
(f) n = 8.

Figure 4.- Concluded.
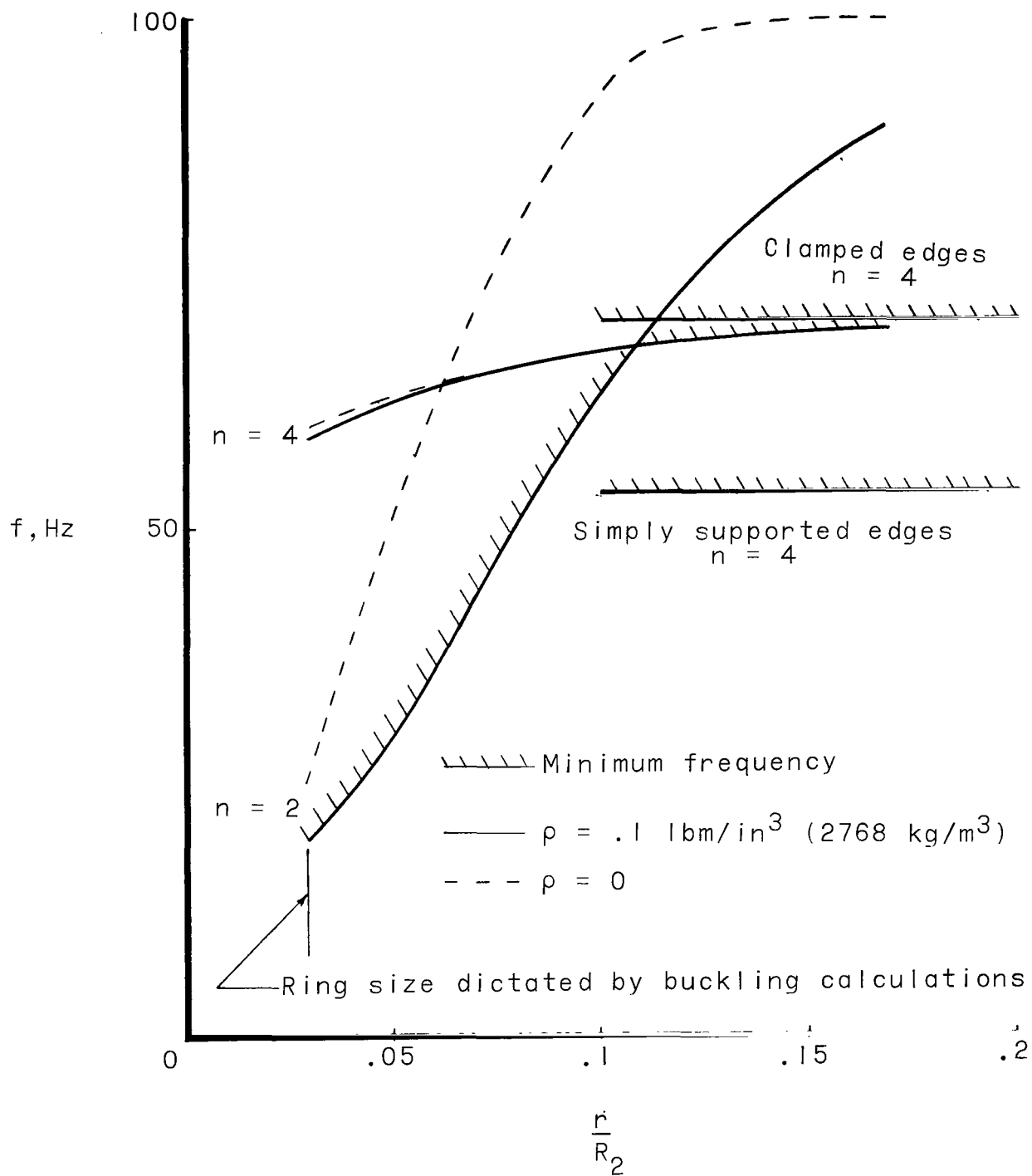
Figure 5.- Effect of base-ring size on free-vibration characteristics of shell A.
r/t = 34.4. (See fig. 1 for shell geometry.)

(a) $\frac{r}{R_2} = 0.0294$.

(b) $\frac{r}{R_2} = 0.0555$.

(c) $\frac{r}{R_2} = 0.1670$.
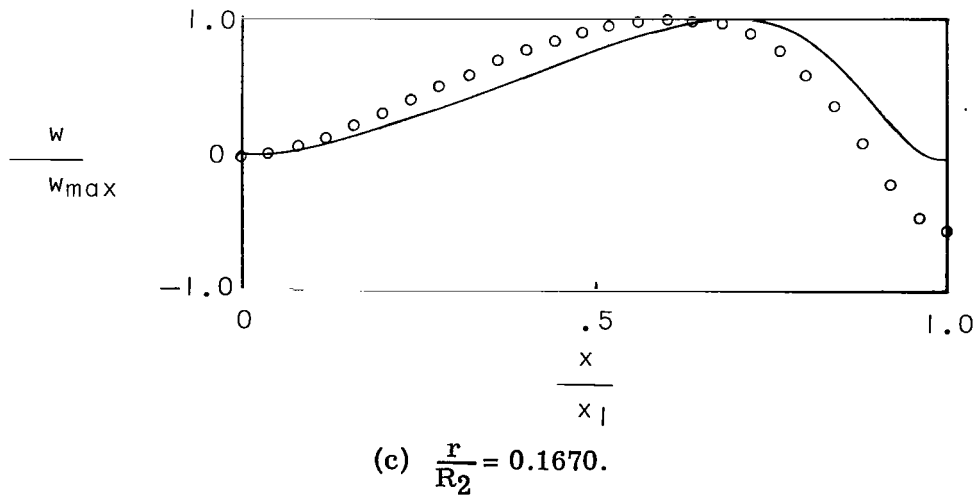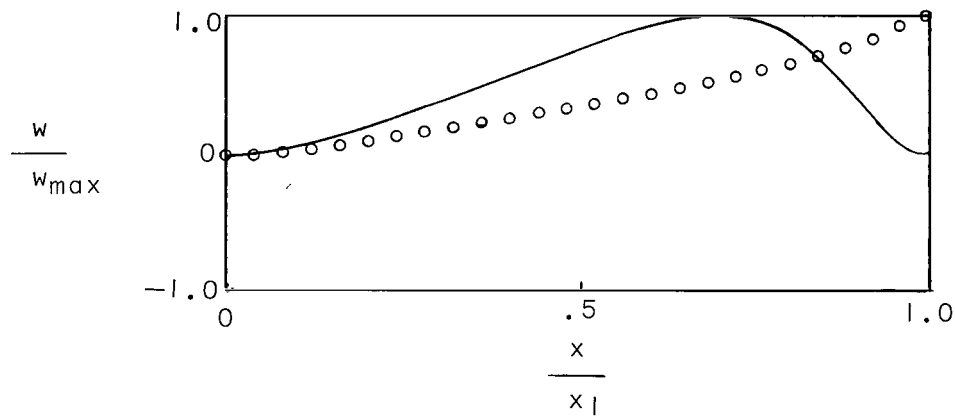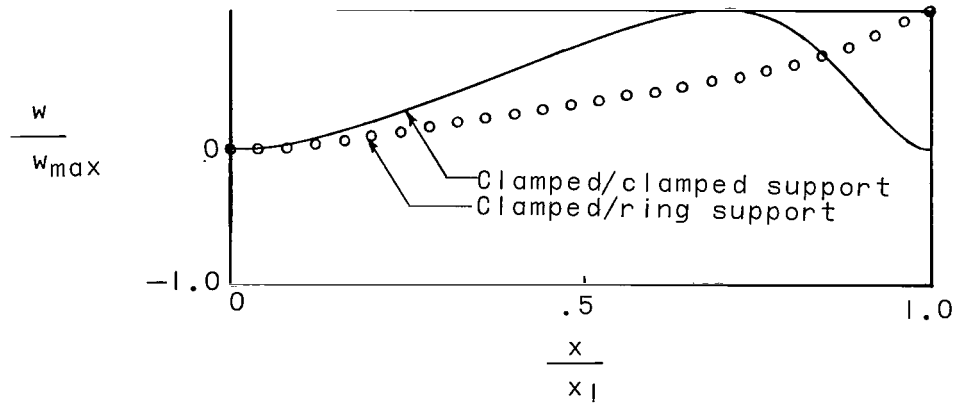
Figure 6.- Variation of vibration mode shapes with
base-ring size for shell A. n = 2.

Material Properties

E		ρ		μ
psi	GN/m^2	lbm/in^3	kg/m^3	
6.4 x 10^6	44.1	0.064	1772	.35

Model Dimensions

α	R_1		R_2		h	
	in.	cm	in.	cm	in.	cm
60°	3.93	9.98	10	25.4	.076	.193
70°	3.93	9.98	10	25.4	.085	.216

Ring Properties

α	Ring	$\bar{A}$	$\bar{I}_z$	$\bar{I}_y$	$\bar{I}_{yz}$	$\bar{J}$	$\bar{\rho}$	z_o/R_2
60°	1	.4290	.00382	.00039	.00053	.00108	.4889	.0155
60°	2	.5352	.00574	.00066	.00097	.00105	.6100	.0157
70°	1	.3719	.00347	.00063	.00130	.00112	.4238	.0168
70°	2	.4502	.00489	.00098	.00106	.00108	.5131	.0170

Figure 7.- Construction details of test models.

Support vanes

Sting

Sting support

Blunt conical shell
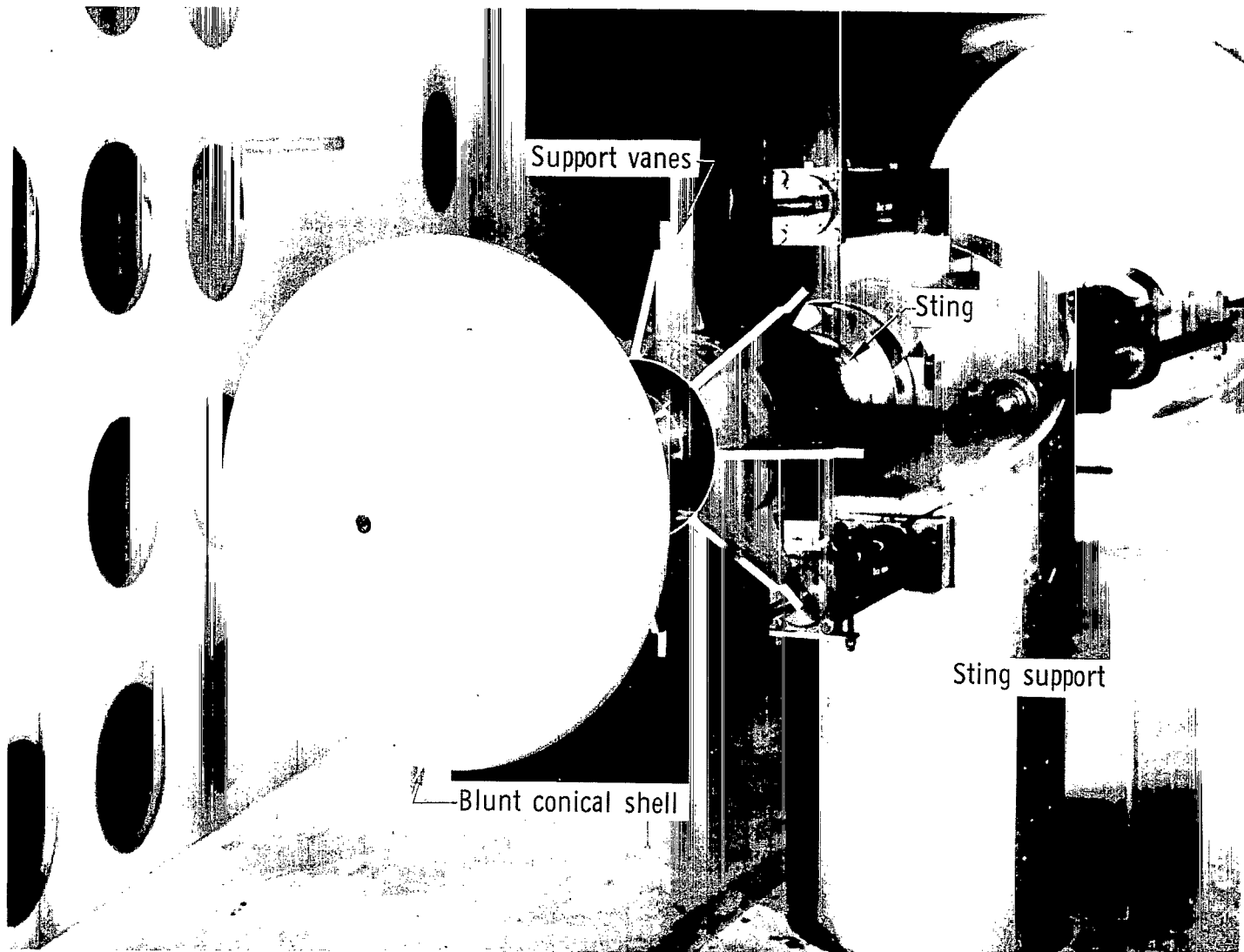
L-68-9859.1

Figure 8.- Model in wind-tunnel test section.

27

(a) Ring 1, $\alpha = 120^O$.
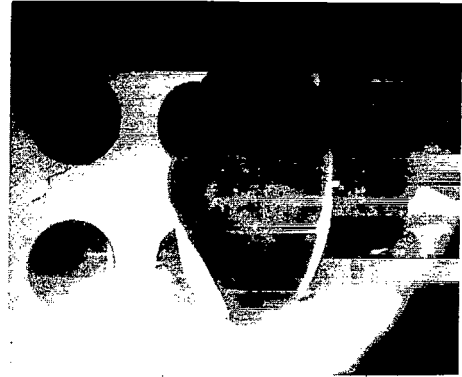
(b) Ring 2, $\alpha = 120^O$.

(c) Ring 1, $\alpha = 140^O$.
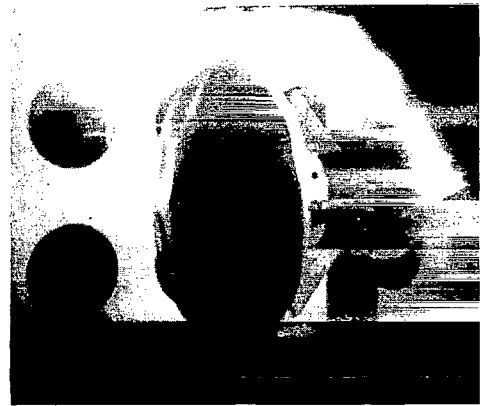
L-70-4786

(d) Ring 2, $\alpha = 140^O$.

Figure 9.- Initial deformations in test models induced by
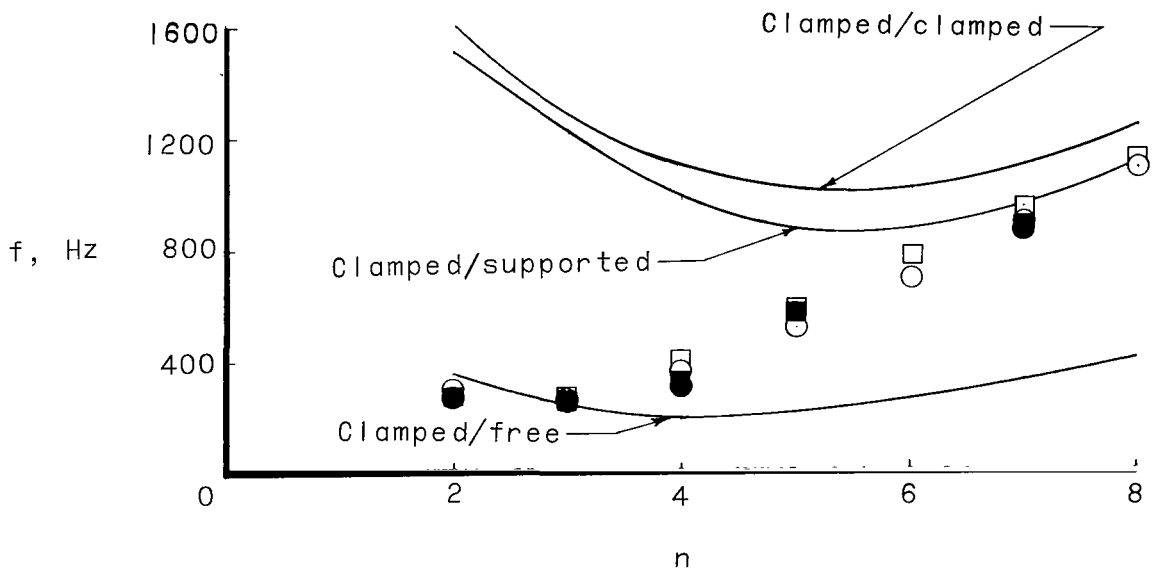buffeting during tunnel startup.

CENTIMETERS
INCHES

L-69-7020

Figure 10.- Test model after collapse into $n = 3$ mode.
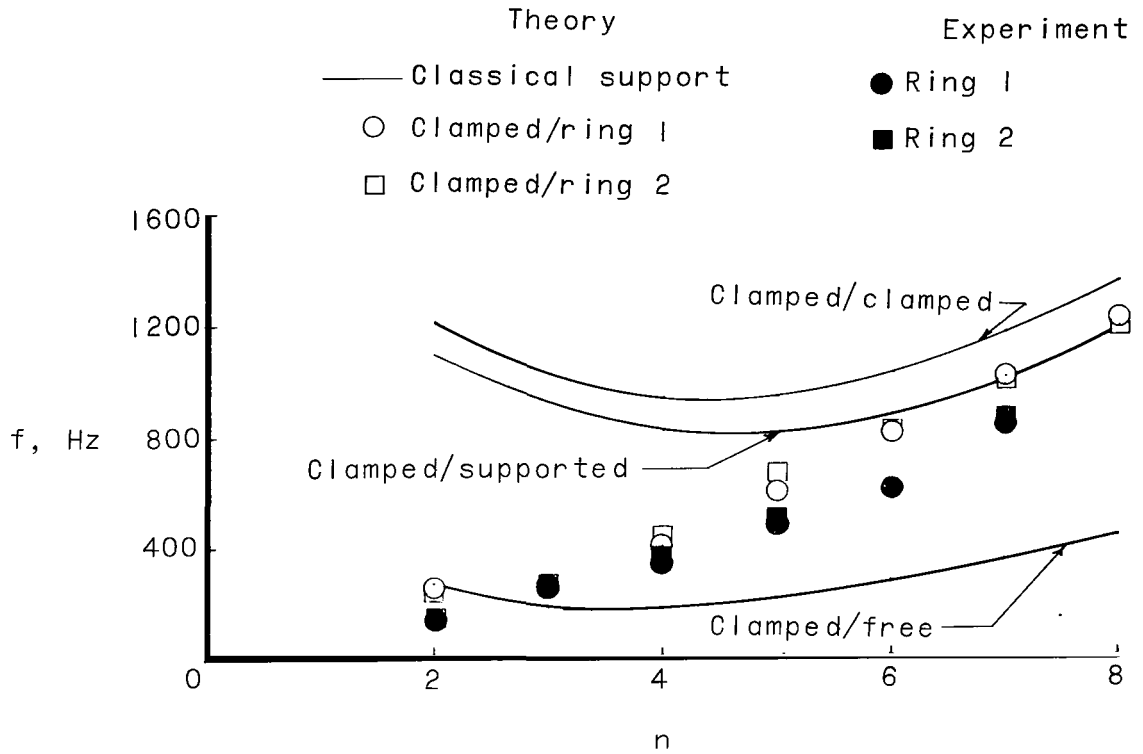
(a) 120° cone.

(b) 140° cone.

Figure 11.- Comparison of theoretical and experimental vibration results for blunt conical shells clamped at small end and ring-supported at large end.
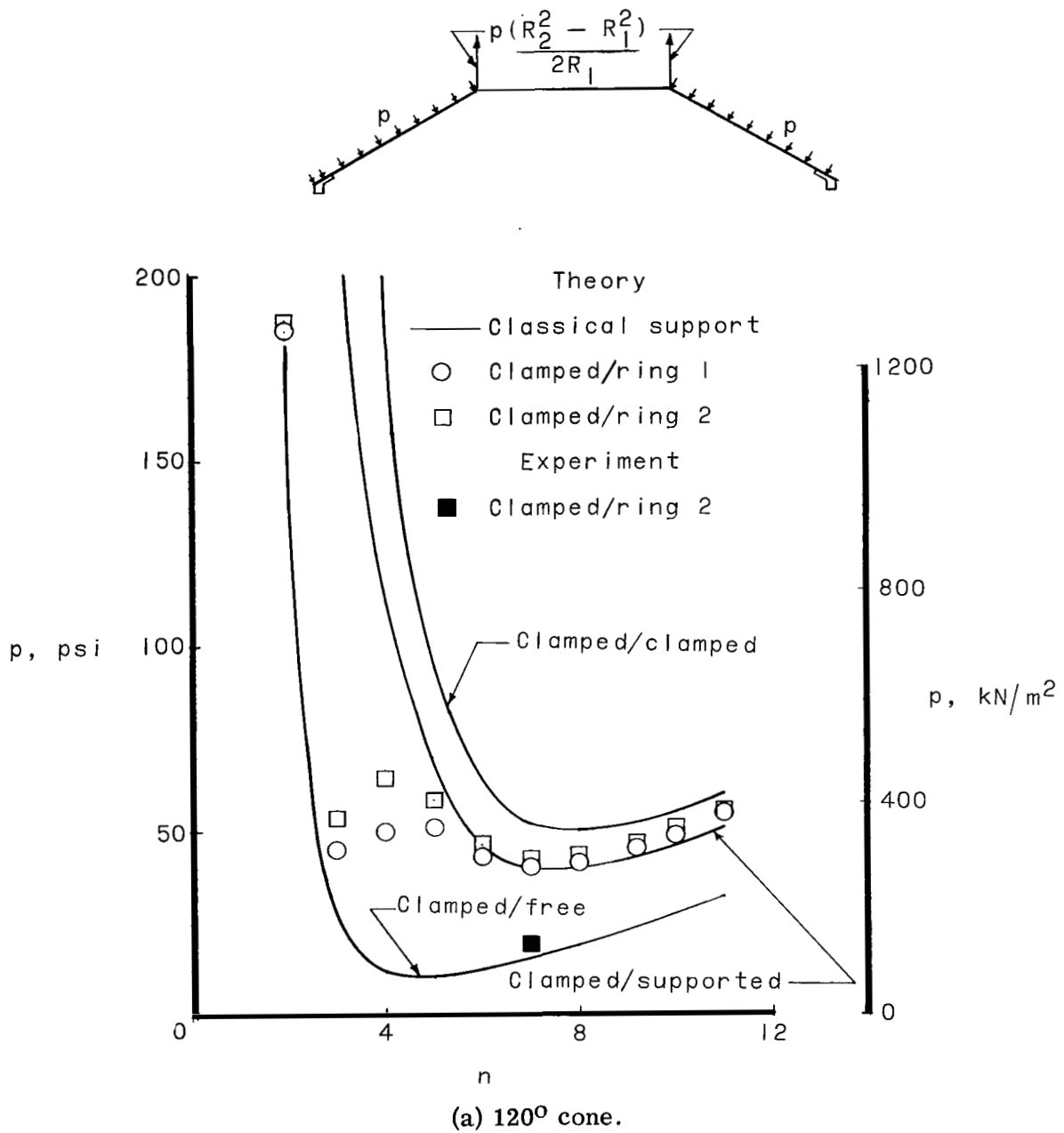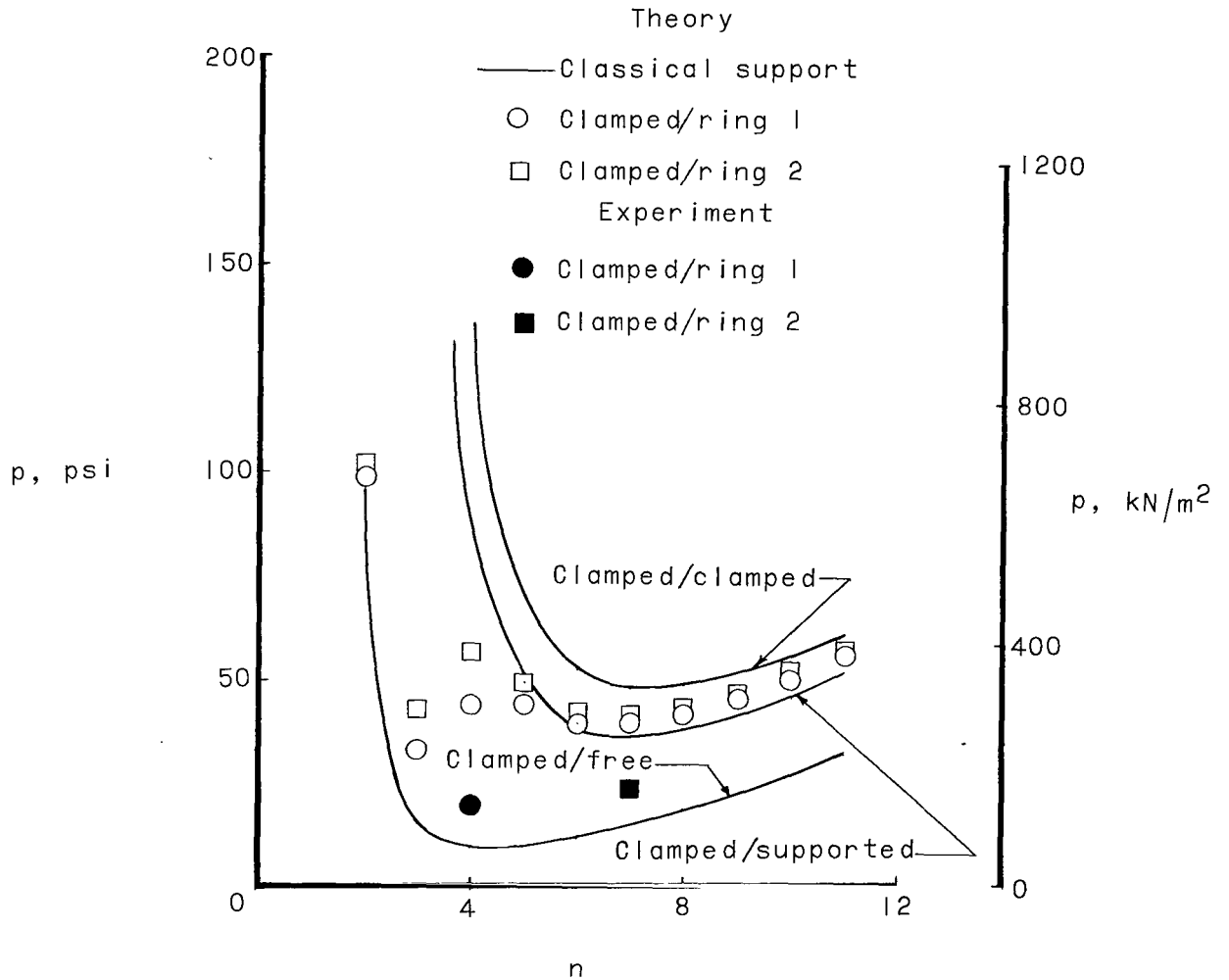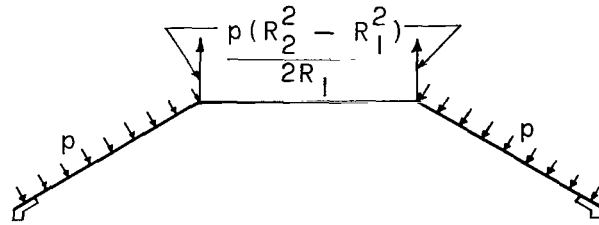
(a) 120° cone.

Figure 12.- Comparison of theoretical and experimental buckling results for blunt conical shells clamped at small end and ring-supported at large end.

$$\frac{p(R_2^2 - R_1^2)}{2R_1}$$

(b) 140° cone.

Figure 12.- Concluded.